Heats of Formation of the Propionyl Ion and Radical and 2,3-Pentanedione by Threshold Photoelectron Photoion Coincidence Spectroscopy

James P. Kercher,[†] Elizabeth A. Fogleman,[†] Hideya Koizumi,[†] Bálint Sztáray,[‡] and Tomas Baer*,[†]

Department of Chemistry, University of North Carolina, Chapel Hill, North Carolina 27599-3290, and Department of General and Inorganic Chemistry, Eötvös Loránd University, Budapest, Hungary

Received: September 14, 2004; In Final Form: November 19, 2004

The dissociative photoionization onsets for the formation of the propionyl ion ($C_2H_5CO^+$) and the acetyl ion (CH_3CO^+) were measured from energy selected butanone and 2,3-pentanedione ions using the technique of threshold photoelectron photoion coincidence (TPEPICO) spectroscopy. Ion time-of-flight (TOF) mass spectra recorded as a function of the ion internal energy permitted the construction of breakdown diagrams, which are the fractional abundances of ions as a function of the photon energy. The fitting of these diagrams with the statistical theory of unimolecular decay permitted the extraction of the 0 K dissociation limits of the first and second dissociation channels. This procedure was tested using the known energetics of the higher energy dissociation channel in butanone that produced the acetyl ion and the ethyl radical. By combining the measured dissociative photoionization onsets with the well-established heats of formation of $CH_3^•$, CH_3CO^+, $CH_3CO^•$, and butanone, the 298 K heats of formation, $\Delta_f H°_{298K}$, of the propionyl ion and radical were determined to be 618.6 ± 1.4 and −31.7 ± 3.4 kJ/mol, respectively, and $\Delta_f H°_{298K}$[2,3-pentanedione] was determined to be −343.7 ± 2.5 kJ/mol. This is the first experimentally determined value for the heat of formation for 2,3-pentanedione. Ab initio calculations at the Weizmann-1 (W1) level of theory predict $\Delta_f H°_{298K}$ values for the propionyl ion and radical of 617.9 and −33.3 kJ/mol, respectively, in excellent agreement with the measured values.

Introduction

Establishing the heats of formation of radicals, ions, and neutrals by measuring dissociative photoionization onsets is based on the following reaction:

$$AB + h\nu \rightarrow A^+ + B \qquad (1)$$

in which the heats of formation of the three species are related to the threshold energy, E_0, by the thermochemical cycle:

$$E_0 = \Delta_f H°[A^+] + \Delta_f H°[B] - \Delta_f H°[AB] \qquad (2)$$

The ideal reaction should meet several criteria, among which are the following: (a) there should be no activation energy for the reverse reaction, (b) the heats of formation of two of the three species must be well established, and (c) the reaction of interest should in general be the lowest energy dissociation channel. The last requirement is a result of the so-called competitive shift,[1−3] which shifts the observed onset for a higher energy channel to higher energies. This is because, at the dissociation limit for the second channel, the rate of the lowest energy reaction may be orders of magnitude higher than the rate of the second reaction, thereby preventing the observation of products at the dissociation limit. In this paper, we utilize the statistical theory of unimolecular decay[4] to model the experimental data for higher energy dissociation channels in order to remove this last limitation associated with the photoionization method. The benefit of this analysis is the ability to investigate new species not otherwise accessible.

We have recently studied the heats of formation of the acetyl radical ($CH_3CO^•$) and ion (CH_3CO^+) through the photoionization of acetone and butanedione.[5] In the present study, we use two starting molecules and three reactions to establish the heats of formation of the propionyl radical ($C_2H_5CO^•$), the propionyl ion ($C_2H_5CO^+$), and 2,3-pentanedione ($C_2H_5COCOCH_3$). The reactions involved are the following:

$$C_2H_5COCH_3 + h\nu \rightarrow C_2H_5CO^+ + CH_3^• \qquad (3a)$$

$$\rightarrow CH_3CO^+ + C_2H_5^• \qquad (3b)$$

$$C_2H_5COCOCH_3 + h\nu \rightarrow C_2H_5CO^+ + CH_3CO^• \qquad (4a)$$

$$\rightarrow CH_3CO^+ + C_2H_5CO^• \qquad (4b)$$

The heat of formation of butanone is known to within 1 kJ/mol, as are the heats of formation of $CH_3^•$, $C_2H_5^•$, CH_3CO^+, and $CH_3CO^•$.[5] With the aid of velocity focusing optics for electrons and a method for the subtraction of the "hot" electron contamination in the threshold signal,[6] we are now able to determine the first dissociation onsets to within 1 kJ/mol and the second dissociation onsets to within 2 kJ/mol. The propionyl ion production channels (3a and 4a) are the lowest energy dissociation channels, whereas the acetyl ion production channels (3b and 4b) are the second lowest energy dissociation channels. We can test our ability to extract the second onset energies by using the known thermochemistry of reaction 3b.

The onset of the $C_2H_5CO^+$ ion from butanone (reaction 3a) was investigated some years ago by Murad and Inghram[7] as

[†] University of North Carolina.
[‡] Eötvös Loránd University.

10.1021/jp0458497 CCC: $30.25
Published on Web 01/19/2005

TABLE 1: Vibrational Frequencies Calculated at the B3LYP/6-311++G Level**

$CH_3COC_2H_5$	53, 102, 198, 247, 401, 475, 590, 753, 762, 941, 955, 1000, 1105, 1129, 1185, 1284, 1370, 1387, 1417, 1453, 1467, 1497, 1492, 1500, 1783, 3007, 3028, 3031, 3041, 3085, 3103, 3112, 3137
$CH_3COC_2H_5^+$	53, 117, 228, 239, 340, 404, 470, 565, 742, 806, 938, 966, 1014, 1063, 1078, 1246, 1279, 1335, 1406, 1426, 1428, 1449, 1454, 1491, 1695, 3008, 3028, 3035, 3082, 3099, 3121, 3141, 3177
$C_2H_5COCOCH_3$	38, 53, 102, 190, 207, 259, 366, 414, 520, 538, 660, 715, 808, 904, 977, 1001, 1045, 1083, 1147, 1247, 1301, 1333, 1389, 1405, 1456, 1458, 1470, 1500, 1507, 1775, 1780, 3036, 3041, 3056, 3097, 3097, 3106, 3119, 3149
$C_2H_5COCOCH_3^+$	16, 45, 99, 174, 189, 209, 230, 328, 394, 456, 487, 620, 800, 814, 892, 945, 1017, 1036, 1058, 1101, 1260, 1289, 1366, 1413, 1427, 1441, 1453, 1486, 1496, 1985, 1997, 3040, 3053, 3058, 3114, 3122, 3128, 3144, 3148
CH_3CO^+	418, 418, 910, 1028, 1028, 1363, 1396, 1396, 2385, 2999, 3080, 3081
$C_2H_5CO^+$	188, 193, 419, 599, 771, 833, 930, 1069, 1099, 1252, 1271, 1403, 1422, 1487, 1493, 2352, 3007, 3047, 3068, 3154, 3162
CH_3CO	110, 469, 855, 956, 1049, 1358, 1453, 1457, 1925, 3016, 3108, 3114
C_2H_5CO	105, 234, 237, 625, 729, 799, 973, 1047, 1081, 1267, 1316, 1410, 1445, 1493, 1499, 1917, 3039, 3039, 3064, 3106, 3114
CH_3	537, 1402, 1402, 3102, 3282, 3282
C_2H_5	98, 489, 813, 978, 1062, 1190, 1399, 1463, 1481, 1481, 2943, 3034, 3078, 3141, 3241

well as by Traeger[8] and revisited very recently by Harvey and Traeger.[9] The latter study yielded a $\Delta_f H°_{298K}[C_2H_5CO^+]$ value of 617.8 ± 0.9 kJ/mol. In a later paper, Murad and Inghram[10] measured the onsets for reaction 4a to be 9.67 eV but did not assign an onset energy for reaction 4b. In the present work, we repeat these measurements and present the first experimentally determined value for the heat of formation of 2,3-pentanedione as well as a new value for the heat of formation of the propionyl radical. We also show that the effects of the competitive shift can be accounted for in the modeling in order to obtain accurate dissociative onsets for higher energy channels. This ability to model higher energy onsets permits us to utilize reactions 4a and b to extract thermochemical values. That is, we can use the measured onset for 4a to obtain the heat of formation of 2,3-pentanedione, which in turn can be used in reaction 4b to yield the heat of formation of the propionyl radical from the higher energy onset.

Experimental Approach

The threshold photoelectron photoion coincidence (TPEPICO) apparatus has been described in detail elsewhere.[5,6,11] Briefly, room-temperature sample vapor is introduced into the experimental chamber through a small stainless steel capillary pointing into the ionization region and is then ionized with vacuum ultraviolet (VUV) light from a hydrogen discharge lamp dispersed by a 1m normal incidence monochromator with a resolution of 12 meV at a photon energy of 10.0 eV. The VUV wavelengths are calibrated by using the Lyman-α emission at 1215.67 Å, which is the most intense line in this spectrum. The ions and electrons are extracted in opposite directions with an electric field of 20 V/cm. Electrons pass through a second acceleration region where they are accelerated to a final electron energy of 74 eV. They then drift 13 cm along a field-free drift region. The applied voltages are designed to velocity focus threshold electrons onto a 1.4 mm aperture at the end of the electron drift region, where a Channeltron detects them. At the same time, energetic electrons, focused to a ring around the central hole, are collected by a Burle multichannel plate detector (tandem MCPs) and provide a measure of the hot electron signal. By subtracting a factor of the coincidence spectrum obtained with the MCP from the TPEPICO spectrum, we obtain a TPEPICO spectrum free of hot electron contamination.

The ions are accelerated to 100 eV in the first 5 cm long acceleration region and travel 40 cm in the first drift region. Ions are then reflected and travel through another 35 cm second drift region before being collected at a tandem multichannel plate ion detector. The electron and ion signals are used as start and stop pulses for measuring the ion time-of-flight (TOF). Typical electron and ion count rates are 50 electrons/s and 300 ions/s, so that a complete TPEPICO TOF spectrum could be collected in 2−12 h. The TOF distributions, obtained at each photon energy, are used to obtain the fractional abundance of the precursor and the product ions (breakdown diagram). Both neutral precursors were acquired from Aldrich Chemical Co. and used without further purification. No impurities were detected in the TPEPICO mass spectra.

Theoretical Approach

In support of our data analysis and statistical theory (RRKM) calculations, the geometry and vibrational frequencies of all molecules studied were calculated using Becke 3 parameter exchange[12] with the functional of Lee−Yang−Parr correlation (B3LYP)[13] and the 6-311++G** basis set implemented in the Gaussian 03 program, version B04.[14] The harmonic frequencies of butanone and 2,3-pentanedione were used in the calculation of the neutral internal energy distribution and are listed in Table 1 without scaling. These frequencies were not scaled on the basis of the findings of Magalhaes and Soares Pinto,[15] who found that B3LYP/6-311++G** frequencies should not be scaled. In addition, the analysis of parallel dissociation pathways requires assumptions about the structure of the transition state, so that those frequencies were calculated as well. The transition states for all dissociation pathways were calculated using the B3LYP functional and the 6-311++G** basis.

High-level calculations were performed to determine the heats of formation of the propionyl ion and neutral free radical. The total atomization energy of the propionyl ion and radical are calculated at the Weizmann-1 (W1) level of theory, where computational methods are outlined by Martin and co-workers in detail.[16] Geometry optimization and vibrational frequency calculations have been performed at the B3LYP/cc-pVTZ level using the Gaussian 03 program, version B04.[14] All other calculations were carried out using MOLPRO 2002.3.[17]

Briefly, the self-consistent field (SCF) limit was obtained using a two-point formula[18] using Dunning's augmented correlation consistent n-tuple zeta basis sets, aug-cc-pVTZ (AVTZ) and aug-cc-pVQZ (AVQZ). Closed-shell CCSD[19] with perturbative triple corrections[20] and spin unrestricted RHF-UCCSD-(T) open-shell coupled cluster theories[21] are used to calculate the electron correlation of the propionyl ion and radical, respectively. The T-1 diagnostics[22] for the propionyl radical (0.019) does not suggest a need for a multireference electron correlation procedure. The largest calculations, CCSD/AVQZ, were carried out using the integral-direct algorithm[23] implemented in MOLPRO 2002.3.[17] CCSD and CCSD(T) contributions are obtained using the exponent 3.22 derived from W2 comparison.[16] The core valence correlations are considered at the CCSD(T) level using the core correlation basis set MTsmall.[16] BSSE corrections to core valence correlations[24] are not considered here. Scalar relativistic effects are considered at the

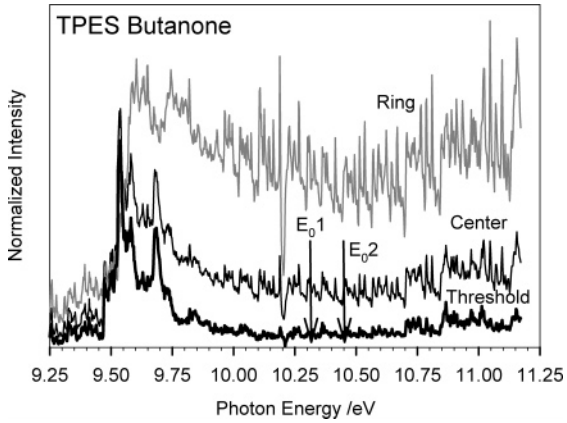

Figure 1. Threshold photoelectron spectrum of butanone from 9.25 to 11.25 eV. The true threshold signal is obtained by subtracting the hot electron contribution (ring) from the center (threshold and hot electron contamination) signal. The adiabatic IE (not marked) was determined to be 9.52 ± 0.04 eV. The dissociation onsets for the propionyl ion, $E_0$1, and the acetyl ion, $E_0$2, are marked. These occur in a Franck−Condon gap.

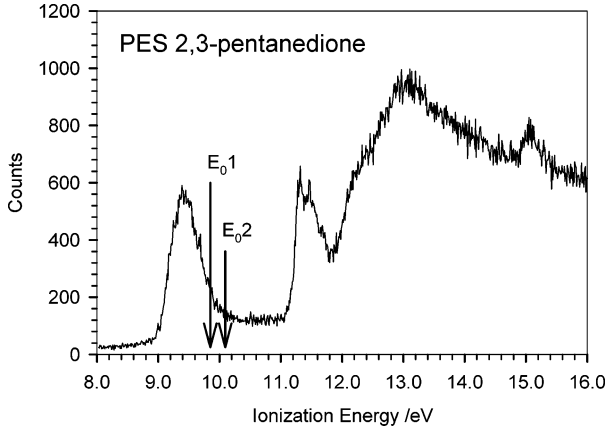

Figure 2. Ultraviolet photoelectron spectrum (UPS) of 2,3-pentanedione in the energy range 8−16.0 eV. The dissociation onsets for the propionyl, $E_0$1, and acetyl, $E_0$2, ions have been marked. The adiabatic IE (not marked) was determined to be 9.10 ± 0.04 eV.

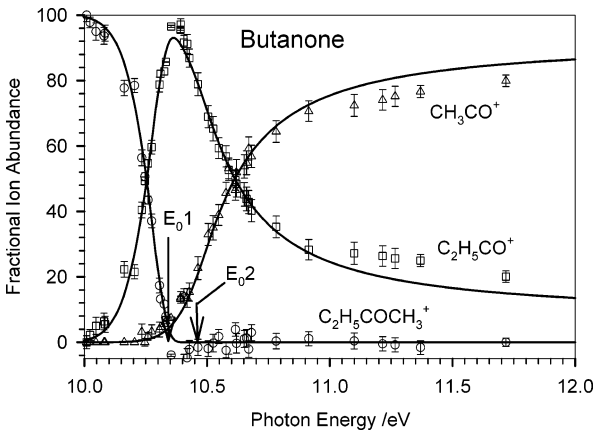

Figure 3. Breakdown diagram of butanone in the range 10.0−12.0 eV. The open points are the experimentally determined ion ratios (circles represent the parent ion, squares represent the propionyl ion, and triangles represent the acetyl ion). The lines are the calculated ion ratios. The dissociation onsets for the propionyl ion, $E_0$1, and the acetyl ion, $E_0$2, are marked.

averaged coupled pair functional (ACPF)[25] with the MTsmall basis set, which gives essentially the same results as the more accurate one-electron Douglas−Kroll approximation[26,27] at the CCSD(T)/MTsmall level (only 0.2 kJ/mol difference for propionyl radical). Spin−orbit coupling is taken into account from CODATA.[28] The resulting atomization energy is converted into the heat of formation using the standard formula. The adiabatic ionization energy (IE) is given by the 0 K atomization energy difference between the cation and neutral at their optimized geometries.

Results and Data Analysis

Photoelectron Spectra. The threshold photoelectron spectrum (TPES) of butanone was obtained by scanning the photon energy while collecting the zero energy electrons. A fraction of the ring signal (hot electrons) was subtracted from the central electrode signal to yield the true TPES shown in Figure 1. The factor is the same in the breakdown diagram and the TPES. The derived dissociation onsets are indicated with a vertical arrow. It is apparent that the dissociation limits lie in a Franck−Condon gap, which means that the production of threshold electrons in the region of the dissociation limit is very small. The true threshold electron signal collected at the center electrode comprised only a small portion of the total signal, resulting in a very low yield of the propionyl ion signal. The first TPES band of butanone is rather broad, making the assignment of the adiabatic ionization energy difficult. The adiabatic ionization energy was determined to be 9.52 ± 0.04 eV.

Uninteresting technical difficulties prohibited the collection of the TPES of 2,3-pentanedione. Instead, we show in Figure 2 the ultraviolet photoelectron spectrum (UPS) recorded using the ATOMKI ESA 32 instrument, which has been described in detail elsewhere.[29] The instrument is equipped with a Leybold-Heraeus UVS 10/35 high-intensity gas discharge photon source. The UPS is obtained by ionizing the neutral precursor using a 21.217 eV He(I) lamp and scanning the energy of the ejected photoelectrons. Electrons were collected using a hemispherical energy analyzer, which has a resolution on the order of 25 meV. The spectrum was calibrated using the Ar $^2P_{3/2}$ peak. The dissociation onsets for both the propionyl and acetyl ions occur at the end of the first band, where the yield of threshold electrons, although not massive, was nevertheless greater than in the case of butanone. Here, the adiabatic ionization energy was determined to be 9.10 ± 0.04 eV, which is in agreement with the value obtained from the photoionization efficiency measurements of Murad and Inghram.[10]

Threshold Photoelectron Photoion Coincidence. *Butanone.* Time-of-flight mass spectra were recorded in the photon energy range from 10.0 to 12.0 eV. The breakdown diagram, given in Figure 3, is a plot of the ratios of the integrated peak areas for each ion as a function of the photon energy. The breakdown diagram was corrected for the hot electron contamination, which has been described in detail elsewhere.[5,11] At low energies, only the parent ion is observed. The first dissociation pathway is associated with the methyl loss channel producing the propionyl cation. At a slightly higher ion energy, the ethyl loss channel producing the acetyl ion appears. The open points represent the experimentally determined ratios of the ion abundances, while the lines represent the calculated ratios.

The time-of-flight (TOF) distributions of the propionyl ion ($C_2H_5CO^+$) fragments obtained from butanone were symmetric, which indicates that the products are formed via rapid reactions with rate constants in excess of 10^7 s^{-1}. The symmetric peaks mean that the observed onset for the first dissociation channel is not shifted to higher energy by the kinetic shift associated with slowly dissociating ions.[1−3]

Because the propionyl ion production is fast, the breakdown diagram for this lowest energy dissociation channel can be modeled with just the thermal energy distribution of neutral butanone. We assume that if the total internal energy of an ion ($h\nu - \mathrm{IE} + E_{th}$, where E_{th} is the thermal energy of the precursor molecule) exceeds the dissociation limit, it will dissociate instantly. If the sample were at 0 K where the thermal energy distribution is a delta function, the breakdown diagram would exhibit a step at the dissociation limit. The 298 K thermal energy distribution, $P(E)$, broadens this step toward the low-energy side. We can calculate the parent and daughter ion curves, $B_p(h\nu)$ and $B_d(h\nu)$, respectively, by integrating this distribution as shown in eqs 5 and 6.

$$B_p(h\nu) = \int_0^{E_0 - h\nu} P(E)\, dE \tag{5}$$

$$B_d(h\nu) = \int_{E_0 - h\nu}^{\infty} P(E)\, dE \tag{6}$$

The thermal ro-vibrational energy distribution at 298 K was calculated using vibrational frequencies obtained at the B3LYP/6-311++G** level of theory. For this reaction, the only adjustable parameter is the 0 K dissociation onset, which was found to be 10.353 ± 0.012 eV. The degree of uncertainty, determined by varying E_0 until the fit was noticeably worse, is limited by the scatter in the data and the photon resolution of 12 meV. This 0 K dissociation limit is very close to the onset measured recently by Harvey and Traeger,[9] whose reported 298 K appearance energy in their photoionization experiment converts to 10.347 ± 0.003 eV at 0 K. The 0 K extrapolated Murad and Ingrahm[7] value is 10.37 eV.

The modeling of the higher energy acetyl ion onset is somewhat more involved. Unlike the calculation of the breakdown diagram for the lowest energy reaction, the calculation of the second channel requires some assumptions about the transition states for the two competing reactions. The fractional abundance of the two products above the onset energy of the second product is directly proportional to the ratio of the rate constants for their production. These rates are given by the RRKM statistical theory as

$$k(E) = \frac{N^{\#}(E - E_0)}{h\rho(E)} \tag{7}$$

where $N^{\#}(E - E_0)$ is the sum of the internal energy states of the transition state between 0 and $E - E_0$, h is Planck's constant, and $\rho(E)$ is the density of states of the molecular ion. The production of the propionyl and acetyl ions proceeds from the same molecular ion; therefore, their rates differ only through the numerator of eq 7. Thus, the ratio of their rate constants is given by the ratio of the sum of states of the transition states, as illustrated by

$$\frac{k_1(E)}{k_2(E)} = \frac{N^{\#}{}_1(E - E_1)}{N^{\#}{}_2(E - E_2)} \tag{8}$$

It can be readily appreciated that when the energy of the ion is just equal to E_2, there is only one path for dissociation to the acetyl ion (i.e., $N^{\#}{}_2(0) = 1$) but the value of $N^{\#}{}_1(E - E_2) = 10^7$. This means that the acetyl ion signal cannot compete well with the production of the propionyl ion. As a result, the observed onset is shifted to higher energies by the competitive shift. How rapidly the acetyl ion signal catches up with the propionyl signal is a function of the transition state frequencies for the two reactions. Thus, in addition to the onset energy, E_2, we need to vary the transition state frequencies for one species.

The breakdown diagram for the higher energy region was modeled as follows. When either $CH_3^{\bullet}$ or $C_2H_5^{\bullet}$ fragments are lost, a total of six vibrational frequencies are turned into translations or rotations. These frequencies can be identified by carrying out a B3LYP/6-311++G** calculation with the RCO−R′ bond stretched from the optimized length in the molecular ion to 4 Å. The reaction coordinate is then identified by the negative frequency and the other five disappearing frequencies by their low values. We chose to use this set of frequencies for the transition state associated with the propionyl ion production. We then found a similar set of five frequencies for the acetyl ion channel. These five frequencies were varied along with the onset energy, E_2, until the calculated breakdown diagram agreed with the experimental points. Error limits were obtained by varying the frequencies and calculating new best values for the onset energy. The resulting onset energy is 10.475 ± 0.016 eV for the acetyl ion. Murad and Inghram[7] list this value as 10.5 eV, with the lack of significant figures reflecting their level of confidence in obtaining an onset from a slowly rising signal.

This second onset, along with the established heats of formation of butanone and $C_2H_5^{\bullet}$, was used to determine an acetyl ion heat of formation of 665.3 ± 1.8 kJ/mol, which is in agreement with our previously reported value of 666.7 ± 1.1 kJ/mol.[5] Although the first dissociation in acetone involves the loss of methane, it is a slow reaction that proceeds via tunneling. This channel is effectively blocked once the acetone ion internal energy is above the methyl loss channel because the latter is a fast reaction. Thus, the onset for the methyl loss channel in acetone, which leads to the acetyl ion, can be determined with high precision. The acetyl ion heats of formation obtained from the dissociative ionization of acetone and butanone agree to within 1.4 kJ/mol, which shows that our modeling correctly accounts for the competitive shift associated with higher energy dissociations. This is important to establish because we use this approach for determining the heat of formation of the propionyl radical from the higher energy dissociation pathway in 2,3-pentanedione.

2,3-Pentanedione. As shown in eqs 4a and b, the 2,3-pentanedione ion dissociates to yield the propionyl ion and at somewhat higher energy the acetyl ion. The breakdown diagram for 2,3-pentandione has been constructed in the same manner as described above. A typical TOF distribution is illustrated in Figure 4, and the breakdown diagram is shown in Figure 5. The slightly asymmetric propionyl ion peak in the TOF distribution at ~81.5 μs indicates that this reaction is slow near the dissociation limit. Slow reactions that form products as the parent ions are accelerating in the 5 cm long acceleration region result in asymmetric TOF peaks. Whereas the breakdown diagram is a plot of the relative rate constants over the entire energy range, the absolute rate constant can be extracted from asymmetric TOF profiles.

The TOF distributions and the breakdown diagram for the propionyl ion onset can be modeled by varying the onset energy and the transition state frequencies. This second adjustable parameter is a direct result of the asymmetric TOF distributions, where the lowest five frequencies of the transition state are fit to the experimentally determined rate curve.

The simulated TOF distribution matches the fast and metastable components nicely, except that a drift peak appears in the simulated TOF distribution which is only weakly present and rather broad in the experimental one. This peak is a result

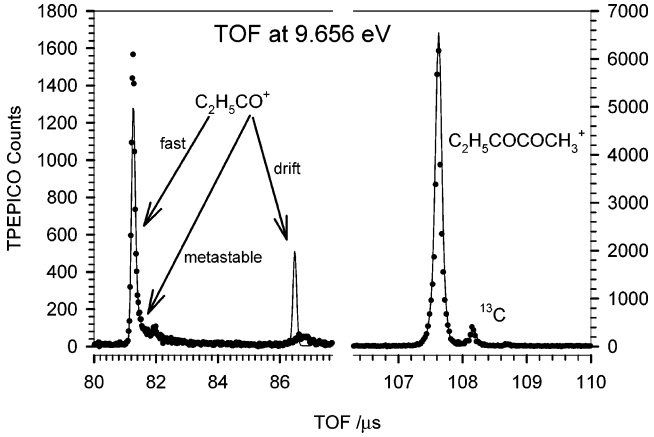

Figure 4. Typical time-of-flight (TOF) distribution for 2,3-pentanedione at a photon energy of 9.656 eV. The points are the experimental counts, while the solid line is the calculated fit. The molecular ion is the peak at ~107.6 μs, and the propionyl ion is at ~81.1 μs. The ^{13}C peak is also present for the propionyl ion and the molecular ion. The simulation indicates the presence of a drift peak; however, no peak is observed experimentally. Note the two different scales.

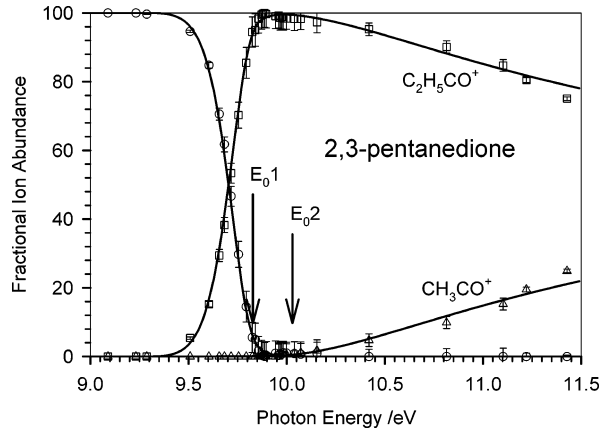

Figure 5. Breakdown diagram of 2,3-pentanedione over the energy range 9.0−11.5 eV. The open points are the experimentally determined ion ratios (circles represent the parent ion, squares represent the propionyl ion, and triangles represent the acetyl ion). The lines are the calculated ion ratios. The dissociation onsets for the propionyl ion, $E_0$1, and the acetyl ion, $E_0$2, are given.

of dissociation in the drift region before the reflectron. The absence of a sharp peak in the experimental TOF distribution is a result of the fact that the reflectron is optimized to pass ions with a certain kinetic energy, namely, parent ions or rapidly produced daughter ions. When the 2,3-pentanedione ion loses the acetyl radical at some time in the drift region before entering the reflectron, the remaining propionyl ion retains just 57% of its initial translational energy. As a result, the daughter ion trajectory is altered as it is being reflected, and therefore, many of these ions never reach the detector. This effect is not noticeable for H or CH_3 loss reactions but becomes increasingly problematic as the neutral mass increases. In the case of 2,3-pentanedione, the energy range for metastable ions goes from the threshold where the minimum rate is 10^2 s^{-1} and rises rapidly to 10^4 s^{-1} within 20 meV. Given that the thermal energy distribution of the molecular ion extends over 200 meV, the metastable ions contribute a negligible fraction to the overall signal. As a result, the error associated with the missing signal near the threshold is minor, as the good fit of the breakdown diagram demonstrates. The fitting of these TOF distributions along with the breakdown diagram yields an onset of 9.841 ± 0.010 eV for the propionyl ion. Murad and Ingrahm[10] obtained a 298 K onset energy of 9.67 eV, which translates to a 0 K onset of ~9.86 eV.

TABLE 2: Ancillary Heats of Formation

species	$\Delta_f H°_{0K}$ (kJ/mol)	$\Delta_f H°_{298K}$ (kJ/mol)	$H°_{298K} - H°_{0K}$
acetyl radical	−3.6 ± 1.8[a]	−9.8 ± 1.8[a]	12.9[b]
acetyl ion	666.7 ± 1.1[a]	659.4 ± 1.1[a]	11.8[b]
butanone	−216.1 ± 0.8[b]	−238.7 ± 0.8[c]	19.8[b]
methyl radical	150.3 ± 0.40[d]	147.1 ± 0.40[d]	10.5[b]
ethyl radical	129.3 ± 0.7[b]	119.0 ± 0.7[e]	13.0[b]
H radical	216.0[f]	218.0[f]	6.12[b]

[a] From Fogleman et al.[5] [b] Conversion calculated by using ab initio vibrational frequencies from Table 1. [c] From IE(butanone) determined in this study and $\Delta_f H°_{298K}$(butanone) taken from Pedley.[48] [d] Determined from $\Delta_f H°_{0K}(CH_3^+)$ from Weitzel et al.[49] and IE(•CH_3) from Blush et al.[50] [e] Private communication from B. Ruscic. Luo[43] lists 118.8 ± 1.3 kJ/mol, and Atkinson et al.[41] lists 120.9 ± 1.6 kJ/mol. [f] From Wagman et al.[30]

With the first onset established, we can keep these parameters fixed and vary the transition state parameters (in order to fit the relative rate constants for the two competing channels) and the onset energy for the second reaction. That is, we assume the extrapolated rate constant for the first dissociation and adjust the second reaction rate to fit the data, as was done for the second reaction in the case of the butanone ion. This yields an onset for the propionyl radical formation of 10.047 ± 0.023 eV. The error is somewhat larger because the onset is less distinct.

Because the two reaction channels differ only in the location of the charge, the difference in the activation energies, $E_2 - E_1$, is equal to the difference in the ionization energies of the two radicals. That is,

$$E_2 - E_1 = \mathrm{IE}[CH_3CO^\bullet] - \mathrm{IE}[C_2H_5CO^\bullet] \qquad (9)$$

which is 0.206 ± 0.025 eV.

Heats of Formation of $C_2H_5CO^+$, $C_2H_5CO^\bullet$, and $C_2H_5COCOCH_3$. The onset energies for reactions 3a, 4a, and 4b along with the ancillary information in Table 2 permit us to derive the heats of formation for the propionyl ion and radical as well as for the neutral 2,3-pentanedione. These values are listed in Table 3. For example, the propionyl ion 0 K heat of formation is related to the dissociation limit by

$$\Delta_f H°_{0K}[C_2H_5CO^+] = E_0 + \Delta_f H°_{0K}[C_2H_5COCH_3] - \Delta_f H°_{0K}[CH_3^\bullet] \qquad (10)$$

which yields a $\Delta_f H°_{0K}[C_2H_5CO^+]$ value of 632.4 ± 1.4 kJ/mol. This value can be converted to 298 K through eq 11:

$$\Delta_f H°_{298K} = \Delta_f H°_{0K} - \sum(H°_{298K} - H°_{0K})_{\mathrm{elements}} + \sum(H°_{298K} - H°_{0K})_{\mathrm{molecule}} \qquad (11)$$

in which the $(H°_{298K} - H°_{0K})_{\mathrm{elements}}$ values are taken from Wagman et al.[30] and the $(H°_{298K} - H°_{0K})_{\mathrm{molecule}}$ values are calculated using the vibrational frequencies in Table 1. This conversion results in a 298 K heat of formation of 618.6 ± 1.4 kJ/mol, which can be compared to the recent Harvey and Traeger value of 617.8 ± 0.9 kJ/mol.[9] The difference in the quoted error limits is probably a subjective matter. In principle, the onset derived by the TPEPICO experiment is more accurate, or at least its interpretation is less subject to uncertainties about transition probabilities and Franck−Condon factors. Neverthe-

TABLE 3: Heats of Formation of $C_2H_5CO^+$, $C_2H_5CO^\bullet$, and $C_2H_5COCOCH_3$

species	$\Delta_fH°_{0K}$[a]	$\Delta_fH°_{298K}$[a]	other experimental $\Delta_fH°_{298K}$	theoretical $\Delta_fH°_{298K}$	$H°_{298K} - H°_{0K}$
propionyl ion	632.4 ± 1.4	618.6 ± 1.4	617.8 ± 0.9[b]	617.9[c] 618[d]	14.9[e]
propionyl radical	−18.0 ± 3.4	−31.7 ± 3.4	−32.3 ± 4.2[f] −34.3 ± 8[g]	−33.3[c]	15.7[e]
2,3-pentanedione	−320.7 ± 2.5	−343.7 ± 2.5		−338.3[h] −348[i]	24.7[e]

[a] From this study. [b] From Harvey and Traeger.[9] [c] W1 calculation from this study. [d] Calculation of Nguyen and Nguyen.[34] [e] Conversion using calculated ab initio vibrational frequencies from Table 1. [f] From Atkinson et al.[41] and Luo[43] based on the kinetic measurements of Watkins and Thompson.[40] [g] Kerr and Lloyd[37] value corrected for the current ethyl radical heat of formation. [h] Isodesmic reaction calculated at the B3LYP/6-311++g** level. [i] Approximation by Pedley, Naylor, and Kirby[46] method.

less, the derived heats of formation clearly agree within the error of the experiments.

Having determined the propionyl ion heat of formation from the butanone dissociation, we can use it and its onset in reaction 4a to determine the heat of formation of 2,3-pentanedione, as listed in Table 3. Finally, we use eq 4b to obtain the propionyl radical heat of formation, $\Delta_fH°_{298K}[C_2H_5CO^\bullet] = -31.7 \pm 3.4$ kJ/mol. The larger error bars are a result of cumulative errors in establishing the 2,3-pentanedione heat of formation and the ±23 meV uncertainty in measuring the second onset.

Theoretical Heats of Formation. To support our calculated heats of formation, we also carried out high-level theoretical atomization energy calculations. The ground state conformers of both the propionyl ion and radical have C_s symmetry at the B3LYP/cc-pVTZ level. Shorter CO and CC bond lengths (1.116 and 1.428 Å) are found for the propionyl ion than for the neutral (1.180 and 1.515A). The OCC bond angle is 178.6 for the propionyl ion. As a consequence of the more rigid structure, the zero-point energy (ZPE) for the ion is higher than that of the neutral by 4 kJ/mol. The ZPEs calculated at this level do not affect the atomization energies even for rigid molecules, as Martin suggested elsewhere.[31] The calculation was tested on the acetyl radical and ion, where we obtained 298 K heats of formation to within 1.3 kJ/mol for the acetyl ion and to within 2.7 kJ/mol for the acetyl radical (the experimental values are given in Table 2). The theoretical heats of formation of the propionyl ion and radical are listed in Table 3. Excellent agreement between theory and experiment is noted for the propionyl ion and propionyl radical in which our calculations differ by only 0.7 and 1.6 kJ/mol from the measured values, respectively. Both of these values are well within the experimental uncertainty of 1.4 and 3.4 kJ/mol.

The heat of formation of the 2,3-pentanedione molecule was also calculated using the following isodesmic reaction:

$$C_2H_5COCOCH_3 + CH_4 \rightarrow CH_3COCOCH_3 + C_2H_6 \quad (12)$$

Because the heats of formation of methane, butanedione, and ethane are all well established, we can use the calculated reaction energy to obtain the heat of formation of the 2,3-pentanedione. These low-cost calculations were carried out using B3LYP/6-311++G** and yielded a $\Delta_fH°_{298}$ value of −338.3 kJ/mol, a value that is close to the −343.7 kJ/mol value obtained from the experiment.

Discussion

$\Delta_fH°_{298K}[C_2H_5CO^+]$ as determined in the present study (618.6 ± 1.4 kJ/mol) and by Harvey and Traeger[9] (617.8 ± 0.9 kJ/mol) is now well established. As pointed out by Harvey and Traeger,[9] the propionyl ion heat of formation can be used to obtain the neutral methyl ketene heat of formation through its proton affinity (eq 12).

$$CH_3CH{=}C{=}O + H^+ \rightarrow C_2H_5CO^+ \qquad \Delta E = PA(CH_3CH{=}C{=}O) \quad (13)$$

Bouchoux and Salpin[32] have determined the proton affinity of methyl ketene to be 839.8 kJ/mol through re-evaluation of thermokinetic measurements, which leads to a methyl ketene $\Delta_fH°_{298K}$ value of −71.6 ± 2.3 kJ/mol. This is an updated value from the Hunter and Lias compilation[33] for which the PA[CH_3-CH=C=O] value was listed as 834.1 kJ/mol and is in better agreement with the theoretical value suggested by Nguyen and Nguyen[34] of 842 kJ/mol. Another route to the neutral heat of formation of methyl ketene is from the appearance energy for the production of ionized phenol and neutral methyl ketene from phenyl propionate, which leads to a value of −66.9 ± 4.7 kJ/mol.[35] However, the phenyl propionate heat of formation, upon which this calculation is based, was estimated.

A final pathway to the heat of formation of methyl ketene is through the photoelectron spectrum of methyl ketene reported by Bock et al.,[36] for which the adiabatic ionization potential was reported to be 8.95 eV. This value can be combined with the $\Delta_fH°_{298K}[CH_3CH{=}C{=}O^+]$ value 783.5 ± 0.3 kJ/mol obtained by Traeger[35] from the averaged values of the appearance energies of $C_3H_4O^+$ from several precursors. This results in a methyl ketene heat of formation of −80.9 ± 1.3 kJ/mol. This value seems out of line with the other two determinations, which led Traeger[35] to suggest that the ionization energy calibration in the photoelectron spectrum of Bock et al. could be off by as much as 0.15 eV. It is evident that the methyl ketene heat of formation remains somewhat controversial.

Kerr and Lloyd[37] first reported a heat of formation of the propionyl radical of −46.0 ± 8 kJ/mol back in 1968 on the basis of the kinetics and pressure dependence of the decomposition of azoethane in the presence of propionaldehyde. Cadman et al.[38] estimated a $\Delta_fH°_{298K}[C_2H_5CO^\bullet]$ value of −41.8 kJ/mol on the basis of the Benson group additivity scheme,[39] which is in good agreement with the experimentally determined value for Kerr and Lloyd. In 1973, Watkins and Thompson[40] studied the addition of ethyl radicals to carbon monoxide to determine the kinetics and thermochemistry of the propionyl radical and, using the slope of an Arrhenius plot, were able to determine a $\Delta_fH°_{298K}[C_2H_5CO^\bullet]$ value of −44.3 kJ/mol. All of the other entries for the propionyl radical heat of formation in various compilations[41−45] are based on these two experiments, although not always directly referenced. A confusion occurred when Lias et al.[44] erroneously listed a $\Delta_fH°_{298K}[C_2H_5CO^\bullet]$ value of +41.5 ± 4 kJ/mol from McMillen and Golden,[42] which was taken from Watkins and Thompson.[40] Unfortunately, the error (it should

TABLE 4: Derived Neutral C−C Bond Energies[a]

species	BDE_{0K} (kJ/mol)	BDE_{298K} (kJ/mol)
$CH_3CH_2CO-COCH_3$	299.1 ± 4.5	302.2 ± 4.5
$CH_3CH_2CO-CH_2CH_3$	336.2 ± 3.5	340.7 ± 3.5
$CH_3CH_2CO-CH_3$	348.4 ± 3.5	354.1 ± 3.5
$CH_3CH_2-COCH_3$	341.8 ± 3.1	347.9 ± 3.0
$CH_3CO-COCH_3$	302.9 ± 2.7	307.2 ± 2.7

[a] The neutral bond energies have been determined for several species on the basis of the heats of formation of $C_2H_5CO^•$, $CH_3CO^•$, $CH_3^•$, and $C_2H_5^•$ listed in Tables 2 and 3 as well as the heats of formation of the molecules taken from Pedley.[48]

have been −41.5 ± 4 kJ/mol) resulted in an IE listing of 5.7 eV, which they obtained from the difference between the propionyl neutral and an old ion heat of formation.[8] Nguyen and Nguyen[34] then used their calculated value for the propionyl ion (see Table 3) and this erroneous IE value to report a radical heat of formation of 68 kJ/mol. In the meantime, the Lias et al. ionization energy has been corrected in the NIST Webbook,[45] where it is listed as 6.6 eV. More recently Atkinson et al.[41] re-evaluated the Watkins and Thompson experimental measurements and, using an updated heat of formation for the ethyl radical, listed a $\Delta_f H°_{298K}[C_2H_5CO^•]$ value of −32.3 ± 4.2 kJ/mol. This is the value that Luo lists in his Handbook of Bond Dissociation Energies.[43] A similarly updated $\Delta_f H°_{298K}[C_2H_5CO^•]$ value of Kerr and Lloyd is −34.3 kJ/mol.

As shown in Table 3, our propionyl radical heat of formation of −31.7 kJ/mol is in good agreement with the previous values based on neutral kinetics as well as our own theoretical calculation. This value depends on two onset measurements for the 2,3-pentanedione ion. The first onset establishes the 2,3-pentanedione heat of formation, and the second onset determines the propionyl radical onset. As already pointed out, the first onset involves a metastable ion anlysis (see fit for asymmetric TOF distribution in Figure 4). Distributions at three ion energies were modeled. Our derived value for the 2,3-pentanedione heat of formation agrees very well with the theoretical value derived from isodesmic reaction 12 as well as that of the Pedley−Naylor−Kirby (PNK) estimation scheme[46] (discussed later).

The propionyl radical heat of formation depends on the second onset. Because the two onsets are so close together (0.206 eV), our precision in measuring this onset is good, as it was in the case of butanone, where we obtained consistent results with the established heat of formation of the acetyl ion and radical. Thus, it is unlikely that the error in our results is beyond 3.5 kJ/mol.

With well-established heats of formation for the propionyl cation and radical, the adiabatic ionization energy for the propionyl radical can be obtained through the following relationship:

$$IE = \Delta_f H°_{0K}[C_2H_5CO^+] - \Delta_f H°_{0K}[C_2H_5CO^•] \quad (14)$$

which yields a value of 6.74 ± 0.04 eV.

The propionyl radical heat of formation can also be used in determining neutral bond energies. These include the C−C bond energies in $CH_3CH_2CO-CH_3$ and $CH_3CH_2CO-COCH_3$, which are summarized in Table 4, along with other derived neutral bond energies such as $CH_3CO-COCH_3$.

The 2,3-pentanedione 298 K heat of formation of −343.7 kJ/mol appears to be the first experimental value reported for this molecule. Such heats of formation are often obtained by group additivity schemes such as that of Benson.[39] The Benson rules work extremely well for determining the heat of formation of butanone, yielding −238 kJ/mol, which is in perfect agreement with the experimental result. (It was probably used to establish the group additivity values.) However, the Benson method yields a $\Delta_f H°_{298K}$[2,3-pentanedione] value of −368 kJ/mol, which is too low by 20 kJ/mol. The group additivity method yields the same −368 kJ/mol value for the isomeric 2,4-pentanedione, whereas the experimentally determined value is −382 kJ/mol.[47] The Benson value is now too high by 14 kJ/mol, but the discrepancy is much less. The method appears to fail due to nearest-neighbor interactions that are not accounted for.

The PNK method[46] for determining the heat of formation is the sum of the contributions of the various components (like the Benson method); however, group interactions are taken into account. When the PNK method is used, a value of −348.4 kJ/mol is obtained for $\Delta_f H°_{298K}$[2,3-pentanedione] and a value of −380.6 kJ/mol is obtained for $\Delta_f H°_{298K}$[2,4-pentanedione]. The value of 2,4-pentanedione agrees extremely well with the experimentally determined value −380 kJ/mol.

Conclusions

The propionyl ion and radical heats of formation have been determined through the photodissociation of butanone and 2,3-pentanedione. The propionyl ion heat of formation agrees with the value determined by Harvey and Traeger[9] as well as with high-level calculations. The acetyl ion heat of formation determined from the second loss channel of butanone agrees with our previously reported value from the lowest energy dissociation in acetone.[5] This indicates that modeling can correctly account for the effects of the competitive shift associated with high energy dissociations. The results also report on the first experimental measurement of the 2,3-pentanedione heat of formation. These values are important in establishing accurate bond dissociation energies for a number of common molecules such as butanone, propanal, and other ketones.

Acknowledgment. We gratefully thank the Department of Energy for the support of this work. One of the authors (B.S.) thankfully acknowledges the generous support of the Magyary Zoltan fellowship.

References and Notes

(1) Chupka, W. A. *J. Chem. Phys.* **1959**, *30*, 191−211.
(2) Huang, F. S.; Dunbar, R. C. *J. Am. Chem. Soc.* **1990**, *112*, 8167−8169.
(3) Lifshitz, C. *Mass Spectrom. Rev.* **1982**, *1*, 309−348.
(4) Baer, T.; Hase, W. L. *Unimolecular Reaction Dynamics: Theory and Experiments*; Oxford University Press: New York, 1996.
(5) Fogleman, E. A.; Koizumi, H.; Kercher, J. P.; Sztáray, B.; Baer, T. *J. Phys. Chem. A* **2004**, *108*, 5288−5294.
(6) Sztáray, B.; Baer, T. *Rev. Sci. Instrum.* **2003**, *74*, 3763−3768.
(7) Murad, E.; Inghram, M. G. *J. Chem. Phys.* **1964**, *40*, 3263−3275.
(8) Traeger, J. C. *Org. Mass Spectrom.* **1985**, *20*, 223−227.
(9) Harvey, Z. A.; Traeger, J. C. *J. Mass Spectrom.* **2004**, *39*, 802−807.
(10) Murad, E.; Inghram, M. G. *J. Chem. Phys.* **1964**, *41*, 404−415.
(11) Koizumi, H.; Baer, T. *J. Phys. Chem. A* **2004**, *108*, 5956−5961.
(12) Becke, A. D. *Phys. Rev. A* **1988**, *38*, 3098−3100.
(13) Lee, C.; Yang, W.; Parr, R. G. *Phys. Rev. B* **1988**, *37*, 785−789.
(14) Frisch, M. J.; Trucks, G. W.; Schlegel, H. B.; Scuseria, G. E.; Robb, M. A.; Cheeseman, J. R.; Montgomery, J. A.; Vreven, T.; Kudin, K. N.; Burant, J. C.; Millam, J. M.; Iyengar, S. S.; Tomasi, J.; Barone, V.; Mennucci, B.; Cossi, M.; Scalmani, G.; Rega, N.; Petersson, G. A.; Nakatsuji, H.; Hada, M.; Ehara, M.; Toyota, K; Fukuda, R.; Hasegawa, J; Ishida, M.; Nakajima, T; Honda, Y.; Kitao, O.; Nakai, H.; Klene, M.; Li, X.; Knox, J. E.; Hratchian, H. P.; Cross, J. B.; Adamo, C.; Jaramillo, J.; Gomperts, R.; Stratmann, F.; Yazyev, O.; Austin, A. J.; Cammi, R.; Pomelli, C.; Ochterski, J. W.; Ayala, P. Y.; Morokuma, K.; Voth, G. A.; Salvador, P.; Dannenberg, J. J.; Zakrzewski, V. G.; Dapprich, S.; Daniels, A. D.; Strain, M. C.; Farkas, Ö.; Malick, D. K.; Rabuck, A. D.; Raghavachari, K.;

Foresman, J. B.; Ortiz, J. V.; Cui, Q.; Baboul, A. G.; Clifford, S.; Cioslowski, J.; Stefanov, B. B.; Liu, G.; Liashenko, A.; Piskorz, P.; Komáromi, I.; Martin, R. L.; Fox, D. J.; Keith, T.; Al-Laham, M. A.; Peng, C. Y.; Nanayakkara, A.; Challacombe, M.; Gill, P. M. W.; Johnson, B.; Chen, W.; Wong, M. W.; Gonzalez, C.; Pople, J. A. *Gaussian 03*, revision A. 1. 2004; Gaussian, Inc.: Pittsburgh, PA, 2004.

(15) Magalhaes, A. L.; Soares Pinto, A. S. *Theor. Chem. Acc.* **2003**, *110*, 70−78.

(16) Martin, J. M. L.; de Oliveira, G. *J. Chem. Phys.* **1999**, *111*, 1843−1856.

(17) The calculations were done with *MOLPRO-2000* (Werner, H. J.; Knowles, P. J.; Almlof, J.; Amos, R. D.; Berning, A.; Cooper, D. L.; Deegan, M. J. O.; Dobbyn, A. J.; Eckert, F.; Elbert, S. T.; Hampel, C.; Lindh, R.; Lloyd, A. W.; Meyer, W.; Nicklass, A.; Peterson, K. A.; Pitzer, R. M.; Stone, A. J.; Taylor, P. R.; Mura, M. E.; Pulay, P.; Schütz, M.; Stoll, H.; Thorsteinsson, T. MOLPRO. Universität Stuttgart, Stuttgart, Germany, University of Sussex, Falmer, Brighton, England, 1997).

(18) Parthiban, S.; Martin, J. M. L. *J. Chem. Phys.* **2001**, *114*, 6014−6029.

(19) Hampel, C.; Peterson, K. A.; Werner, H.-J. *Chem. Phys. Lett.* **1992**, *190*, 1−12.

(20) Watts, J. D.; Gauss, J.; Bartlett, R. J. *J. Chem. Phys.* **1993**, *98*, 8718−8733.

(21) Knowles, P. J.; Hampel, C.; Werner, H.-J. *J. Chem. Phys.* **1993**, *99*, 5219−5227.

(22) Lee, T. J.; Taylor, P. R. *Int. J. Quantum Chem., Quantum Chem. Symp.* **1989**, *23*, 199−210.

(23) Schutz, M.; Roland, L.; Werner, H.-J. *Mol. Phys.* **1999**, *96*, 719−733.

(24) Bauschlicher, C. W., Jr.; Ricca, A. *J. Phys. Chem. A* **1998**, *102*, 8044−8050.

(25) Gdanitz, R. J.; Ahlrichs, R. *Chem. Phys. Lett.* **1988**, *143*, 413−420.

(26) Douglas, M.; Kroll, N. M. *Ann. Phys.* **1974**, *82*, 89−156.

(27) Samzow, R.; Hess, B. A.; Jansen, G. *J. Chem. Phys.* **1992**, *96*, 1227−1231.

(28) Cox, J. D.; Wagman, D. D.; Medvedev, V. A. *CODATA Key Values for Thermodynamics*; Hemisphere Publ. Corp.: New York, 1989.

(29) Sztáray, B.; Szepes, L.; Baer, T. *J. Phys. Chem. A* **2003**, *107*, 9486-9490.

(30) Wagman, D. D.; Evans, W. H. E.; Parker, V. B.; Schum, R. H.; Halow, I.; Mailey, S. M.; Churney, K. L.; Nuttall, R. L. *The NBS Tables of Chemical Thermodynamic Properties, J. Phys. Chem. Ref. Data Vol. 11, Suppl. 2*; NSRDS, U.S. Government Printing Office: Washington, DC, 1982.

(31) de Oliveira, G.; Martin, J. M. L.; Silwal, I. K. C.; Liebman, J. F. *J. Comput. Chem.* **2001**, *22*, 1297−1305.

(32) Bouchoux, G.; Salpin, J. Y. *Rapid Commun. Mass. Spectrom.* **1999**, *13*, 932−936.

(33) Hunter, E. P. L.; Lias, S. G. *J. Phys. Chem. Ref. Data* **1998**, *27*, 413−656.

(34) Nguyen, M. T.; Nguyen, H. M. T. *Chem. Phys. Lett.* **1999**, *300*, 346−350.

(35) Traeger, J. C. *Int. J. Mass Spectrom.* **2000**, *194*, 261−267.

(36) Bock, H.; Hirabayashi, T.; Mohmand, S. *Chem. Ber.* **1981**, *114*, 2595−2608.

(37) Kerr, J. A.; Lloyd, A. C. *Trans. Faraday Soc.* **1967**, *63*, 2480−2488.

(38) Cadman, P.; Dodwell, C.; Trotman-Dickenson, A. F.; White, A. J. *J. Chem. Soc. A* **1970**, 2371−2376.

(39) Benson, S. W. *Thermochemical Kinetics*; John Wiley & Sons: New York, 1976.

(40) Watkins, K. W.; Thompson, W. W. *Int. J. Chem. Kinet.* **1973**, *5*, 791−803.

(41) Atkinson, R.; Baulch, D. L.; Cox, R. A.; Hampson, R. F.; Kerr, J. A.; Rossi, M. J.; Troe, J. *J. Phys. Chem. Ref. Data* **2000**, *29*, 167−266.

(42) McMillen, D. F.; Golden, D. M. *Annu. Rev. Phys. Chem.* **1982**, *33*, 493−532.

(43) Luo, Y.-R. *Handbook of Bond Dissociation Energies in Organic Compounds*; CRC Press: Boca Raton, FL, 2003.

(44) Lias, S. G.; Bartmess, J. E.; Liebman, J. F.; Holmes, J. L.; Levin, R. D.; Mallard, W. G. *Gas Phase Ion and Neutral Thermochemistry, J. Phys. Chem. Ref. Data Vol. 17, Suppl. 1*; NSRDS, U.S. Government Printing Office: Washington, DC, 1988.

(45) Lias, S. G.; Bartmess, J. E.; Liebman, J. F.; Holmes, J. L.; Levin, R. D.; Mallard, W. G. Ion Energetics Data. In *NIST Chemistry WebBook, NIST Standard Reference Database Number 69*; Mallard, W. G., Linstrom, P. J., Eds.; National Institute of Standards and Technology: Gaithersburg, MD, 2000 (http://webbook.nist.gov).

(46) Pedley, J. B.; Naylor, R. D.; Kirby, S. P. *Thermochemical Data of Organic Compounds*; Chapman and Hall: London, 1986.

(47) Hacking, J. M.; Pilcher, G. *J. Chem. Thermodyn.* **1979**, *11*, 1015−1017.

(48) Pedley, J. B. *Thermochemical Data and Structures of Organic Compounds*; Thermodynamics Research Center: College Station, TX, 1994.

(49) Weitzel, K. M.; Malow, M.; Jarvis, G. K.; Baer, T.; Song, Y.; Ng, C. Y. *J. Chem. Phys.* **1999**, *111*, 8267−8270.

(50) Blush, J. A.; Chen, P.; Wiedmann, R. T.; White, M. G. *J. Chem. Phys.* **1993**, *98*, 3557−3559.